This is a repository copy of *Characterization of thick bismuth ferrite-lead titanate films processed by tape casting and templated grain growth*.

White Rose Research Online URL for this paper:
http://eprints.whiterose.ac.uk/89952/

Version: Accepted Version

Article:

Characterization of thick bismuth ferrite-lead titanate films processed by tape casting and templated grain growth

Meghdad Palizdar[1,6], Chris M. Fancher[2], Tim P. Comyn[1], Tim. J. Stevenson[1], Stephen F. Poterala[3], Gary L. Messing[3], Ender Suvaci[4], Annette P. Kleppe[5], Andrew J. Jephcoat[5] and Andrew J. Bell[1]

[1]Institute for Materials Research, University of Leeds, LS2 9JT, Leeds, UK
[2]Department of Materials Science and Engineering, North Carolina State University Raleigh, North Carolina 27695, USA
[3]Department of Materials Science and Engineering, Pennsylvania State University, University Park, 16802,USA
[4]Department of Materials Science and Engineering, Anadolu University, Eskisehir, Turkey
[5]Diamond Light Source Ltd, Diamond House, Harwell Science and Innovation Campus, Didcot, Oxfordshire, OX11 0QX, UK
[6]R&D and Training Department, CPG Industrial, Mining and Technical Services GmbH, Dusseldorf, 40237 Germany

Abstract

The templated grain growth technique was used to synthesize textured $60BiFeO_3$-$40PbTiO_3$ (60:40BFPT). Both Aurivillius ($Bi_4Ti_3O_{12}$, $PbBi_4Ti_4O_{15}$) and perovskite templates ($BaTiO_3$, $SrTiO_3$) were used to prepare 60:40BFPT. Only $BaTiO_3$ templates were found to successful impart a texture to the ceramic matrix. In the case of perovskite templates, ferroelectricity was evident from saturated polarisation hysteresis loops. Saturated polarisation loops were achieved due to the substitution of Ba^{2+} or Sr^{2+}, which reduces the coercive field. $SrTiO_3$ and $BaTiO_3$ templated ceramics showed remanent polarisation of 30 and 36 $\mu C/cm^2$, respectively. Aurivillius templates did not generate ferroelectric materials. Because of their high chemical stability in this system, $BaTiO_3$ templates appear to be the best candidate for fabricating textured BFPT by the reactive templated grain growth method.

1. Introduction

Materials with morphotropic phase boundaries offer the possibility of an electric field induced phase transition, for example as reported by Park [1]. Single crystals such as $Pb(Mg_{1/3}Nb_{2/3})O_3$-$PbTiO_3$ (PMN-PT) and $Pb(Zn_{1/3}Nb_{2/3})O_3$-$PbTiO_3$ (PZN-PT) exhibit considerable electric field induced strain [2-4]. Furthermore, Park showed that this phase transition occurred via polarisation rotation. Complementary neutron and synchrotron x-ray diffraction on PMN-30PT and PZN-8PT revealed that this phase transition occurs through an intermediately monoclinic phase[5]. The orientation of the applied field with respect to the crystal determines the mechanism of rotation of the ferroelectric dipole[6,7].

The solid solution between bismuth ferrite and lead titanate $xBiFeO_3$-$(1-x)PbTiO_3$ or (BFPT) possesses a morphotropic phase boundary (MPB) between the rhombohedral and tetragonal forms at x=0.7, with a spontaneous strain of 18% on the tetragonal side of this boundary[8-12]. The antiferromagnetic Néel temperature drops by approximately 300K on crossing the MPB from the rhombohedral to the tetragonal side [13,14]. It is of interest to investigate the influence of field-driven rhombohedral-tetragonal phase transitions across the MPB in this system, to determine whether correctly oriented BFPT can provide both giant electric field induced strains and significant coupling with the magnetic sub-structure. A field induced transition from rhombohedral to tetragonal phases in textured BFPT could unleash strains as high as the tetragonal spontaneous strain.

Here, we used the template grain growth method (TGG) to synthesis textured BFPT. Both Aurivillius and perovskite plate-like particles were used templates. The texture of templated ceramics was determined using high-energy synchrotron.

2. Experimental Procedure

Aurivillius ($Bi_4Ti_3O_{12}$, $PbBi_4Ti_4O_{15}$) and perovskite ($SrTiO_3$ and $BaTiO_3$) plate-like templates were synthesized using the molten salt method. Details of the molten salt synthesis procedure can be found in Refs 15-19. Templated $0.6BiFeO_3$-$0.4PbTiO_3$ (60:40 BFPT) ceramics were prepared using the reactive template grain growth method. The casting slurry was prepared using the BFPT precursor powder plus 10% by weight of template ($Bi_4Ti_3O_{12}$, $PbBi_4Ti_4O_{15}$, $SrTiO_3$ and $BaTiO_3$), an azeotropic ratio of solvents, binder, plasticizers and dispersant. The slurry was casting by using a shear rate of 512 s^{-1}, achieved by a combination of doctor blade height and speed [16, 17 and 20]. After drying, BFPT templated with $Bi_4Ti_3O_{12}$, $PbBi_4Ti_4O_{15}$, or $SrTiO_3$ were sintered at 1050 °C for 1 hr and BFPT templated with $BaTiO_3$ was sintered at 1100 °C for 1 hr, respectively. The obtained layers are between 0.8 and 1.2 mm thick. To compare the influence of different types of templates on the chemical and physical properties of the material, 60:40 BFPT, using no template, was synthesized as a reference via tape casting and was sintered at 1100 °C for 1 hr.

Scanning electron microscopy (SEM, Zeiss Leo FEG-SEM, Carl Zeiss SMT Ltd.), was used to characterize the grain morphology of templated BFPT. Strain and polarisation measurements where measured using a Radiant LC precision ferroelectric characterization instrument. Dielectric measurements of the sample were carried out using a HP4192A LF impedance analyzer. Synchrotron diffraction was carried out at beam line I15 at the Diamond Light Source facility (Oxfordshire, UK) using hard synchrotron radiation ($\lambda \approx 0.216$ Å). Diffraction data was measured using a 2D image plate (MAR 345). Measured Debye rings were "caked" into individual 2θ-intensity diffraction patterns, at +/- 5° between $\psi = 0°$ and 355°.

3. Results and discussion

3.1. Texture analysis

Table 1. summarizes the dielectric and crystallographic characteristics of 60:40 BFPT synthesised with different templates. It reveals that among those templates, $BaTiO_3$ was able to impose the texture morphology to the matrix, partially. However, there are some drawbacks, such as reduction in Curie temperature (T_c) and c/a ratio.

Table 1. Summary of the crystallographic and dielectric properties of 60:40BFPT made via tape casting using 10 wt.% templates.

Template	Composition	T_c	Permittivity at T_c at 1MHz	c/a ratio	Plate-like textured morphology	Template reaction with the matrix (Impurities)
$Bi_4Ti_3O_{12}$	$Bi_{0.65}Fe_{0.66}Pb_{0.35}Ti_{0.33}O_x$	610 ^{o}C	4500	1.11	-	Completely
$PbBi_4Ti_4O_{15}$	$Bi_{0.66}Fe_{0.59}Pb_{0.35}Ti_{0.41}O_x$	605 ^{o}C	1500	1.10	-	Partially
$SrTiO_3$	$Bi_{0.62}Fe_{0.86}Pb_{0.3}Sr_{0.08}Ti_{0.13}O_x$	360°C	3400	1.01	-	Completely
$BaTiO_3$	$Bi_{0.57}Fe_{0.55}Pb_{0.34}Ba_{0.08}Ti_{0.44}O_x$	574°C	6500	1.03	Partially	partially
No Template	$Bi_{0.62}Fe_{0.59}Pb_{0.38}Ti_{0.40}O_x$	590°C	6200	1.10	-	-

Chemical compositions in Table 1. have been calculated from average EDX spot scan analysis on some parts of samples, ignoring the oxygen content. The SEM micrograph of 60:40BFPT templated with $BaTiO_3$ (Fig. 1) shows a dense microstructure, which consists of both spherical and plate-like regions. The plate-like regions observed in $BaTiO_3$ templated ceramics were not observed in ceramics templated with $Bi_4Ti_3O_{12}$, $PbBi_4Ti_4O_{15}$, or $SrTiO_3$. EDX spectra were measured for various points in both the spherical and plate-like regions to investigate the chemistry of sintered ceramics. Table 2. shows EDX data from different areas of the sample. An inhomogeneous distribution of all cations was observed, particularly Ba^{2+}. The atomic fraction of Ba^{2+} changes from 0.044 to 0.144. Areas rich in Ba^{2+} correspond to locations that formed from reaction between $BaTiO_3$ and the matrix (semi-dissolved templates), whereas regions low in Ba^{2+} suggest regions of the matrix. The EDX data at location 5, in the case of matrix in with low concentration of Ba^{2+}, suggests a formula of $Bi_{0.57}Fe_{0.55}Pb_{0.34}Ba_{0.08}Ti_{0.44}O_x$ which represents Ba-doped 60:40BFPT.
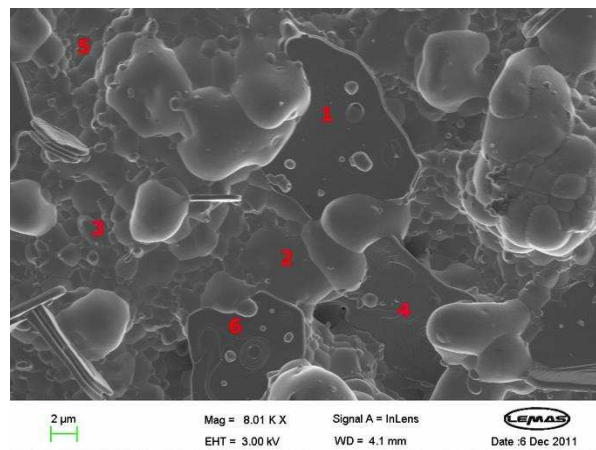
Figure 1. SEM micrograph of the tape-cast plane for a $60BiFeO_3$–$40PbTiO_3$ ceramic templated with 10 wt.% $BaTiO_3$.

Table 2. EDX (atomic fractions) results for 60:40BFPT made from TGG by using 10% $BaTiO_3$ as template.

Elements	Bi (atomic fractions)	Fe (atomic fractions)	Pb (atomic fractions)	Ti (atomic fractions)	Ba (atomic fractions)
1	0.219	0.215	0.149	0.271	0.144
2	0.247	0.252	0.156	0.244	0.098
3	0.302	0.263	0.167	0.218	0.047
4	0.24	0.232	0.164	0.262	0.099
5	0.285	0.274	0.171	0.224	0.044
6	0.253	0.202	0.172	0.264	0.107

In the case of $Bi_3Ti_4O_{12}$ c/a ratio of 1.11 can be calculated from the synchrotron pattern (as mentioned in table 1.) for the tetragonal phase, somewhat lower than that reported by Sai Sunder et al. for 60:40BFPT $\approx$ 1.16[11]. Note that the c/a ratios they calculated were for powders rather than bulk material as presented here. Stevenson [21] reported far lower values from XRD measurement of bulk pellets, prepared via conventional die-pressing, of 1.09, which is commensurate with the values presented here. However, the c/a ratio of $\approx$ 1.033 for BFPT made from $BaTiO_3$ is much lower in comparison with $Bi_3Ti_4O_{12}$ and $PbBi_4Ti_4O_{15}$. This is the evidence for the reaction of the template with the matrix.

Conventional XRD is often insufficient to probe the crystallographic texture of bulk ceramics, due to a material surface being corrupted by (a) reactions with exposed environment and (b) residual stress [22]. In addition, it is challenging to fully characterize angular dependence of the crystallographic texture by conventional XRD. Thus, synchrotron diffraction was used, in order to more effectively probe the texture perpendicular and parallel to the casting direction. Fig. 2 shows the measured synchrotron data for 60:40BFPT made from RTGG method using 10% $BaTiO_3$. The results are compared at about ψ=0 and 90°, where ψ=0° is parallel to the sample normal, and ψ=90° is parallel to the casting direction. The texture was gauged from the difference in the in peak intensities between different angles from 0° to 355°. Comparing the

data at $\psi = 0^o$ and 90° shows a degree of texture, as evidenced by an increase in the intensity of the {00l} at $\psi = 0^o$.
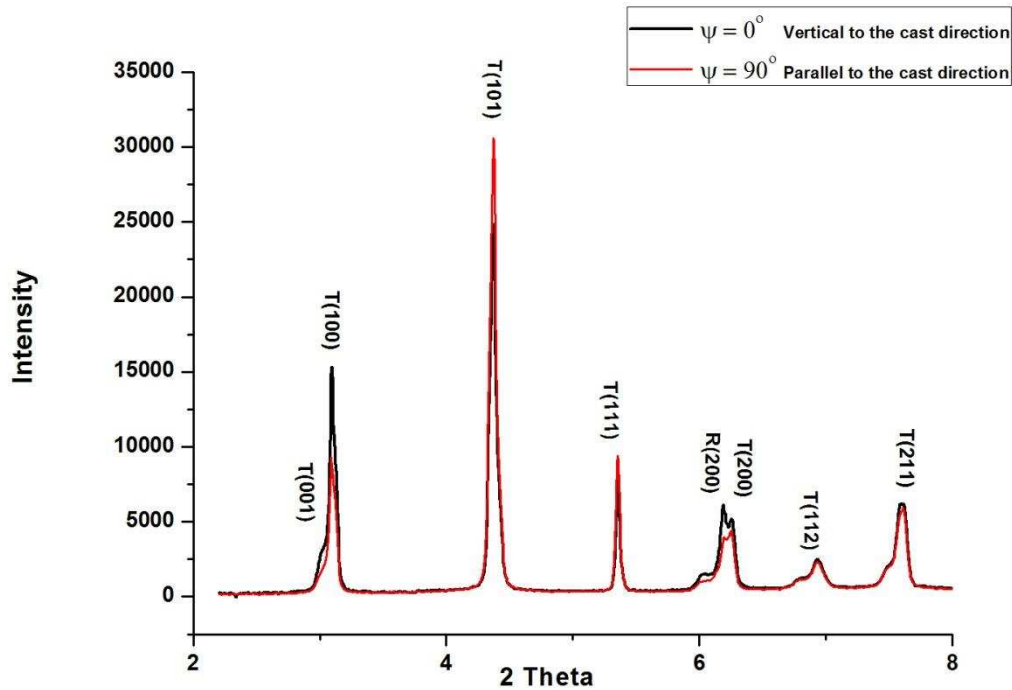
Figure 2. Comparison of synchrotron XRD patterns for 60:40BFPT made from TGG method using 10% $BaTiO_3$ for a scattering vector parallel to the sample normal (ψ=0°) and parallel to the cast direction (ψ=90°).

Fig.3 graphs the angular-dependent (0°< ψ < 360°) diffraction intensity of the 100/001 and 110/011 tetragonal peaks. Fig.3.a shows a large increase at intensity of the (100) tetragonal peak around $\psi = 180°$ and also 0°, normal to the cast direction. Furthermore, two smaller maxima are observed at $\psi = 90°$ and 270°, which are attributed to the formation of 90° domains that form upon cooling through a paraelectric/ferroelectric transition. Fig.3.b shows the maximums for (101) tetragonal peak, which occurs at each 90° period. As expected (101) maximum peaks occur at each 45° period, due to the angle between (001) and (101) planes in

cubic system which is approximately 45°. Similar behaviour is observed for (111) tetragonal peak with much less intense maximum peaks at $\approx 55^{o}$. Comparison the synchrotron results versus different ψ angles for different templates reveals that $BaTiO_3$ is the most successful template.
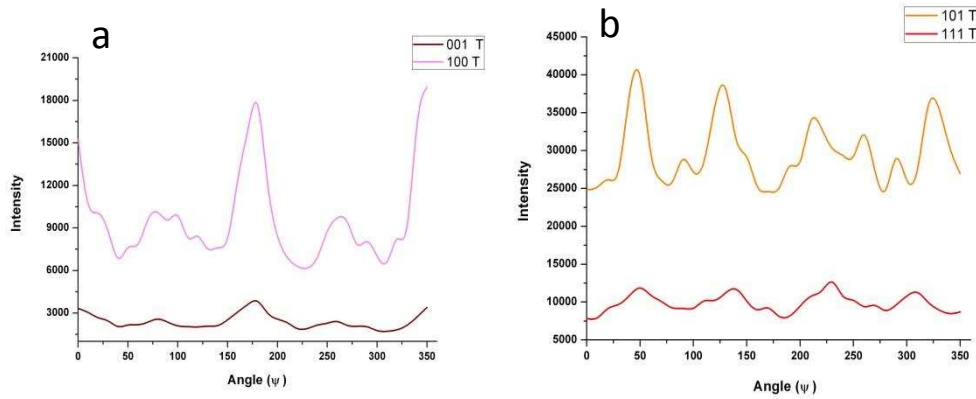
Figure 3. Peak intensity at different ψ angles for a) (100), (001) tetragonal peaks and b) (101), (111) tetragonal peaks for 60:40 BFPT made from 10% $BaTiO_3$.

3.2 Ferroelectric measurements

The electromechanical response of templated 60:40 BFPT is compared to BFPT to assess the effect of texture on the response. Hysteresis loops, as a function of maximum field, measured at 10Hz for 60:40 BFPT made from different templates, can be seen in Fig. 4. It was not possible to collect fully saturated hysteresis loops. However, the materials made using the perovskite templates show strong evidence of ferroelectricity. Remanent polarisation of $2P_r = 60 \, \mu C/cm^2$ at 9.5 kV/mm and $2P_r = 72 \, \mu C/cm^2$ at 7.5 kV/mm were obtained by using $SrTiO_3$ and $BaTiO_3$ as templates, respectively. The high coercive field ($15MVm^{-1}$) of BFPT prevented the measurement of polarisation loops for BFPT and BFPT templated with Aurivillius ($Bi_4Ti_3O_{12}$, $PbBi_4Ti_4O_{15}$)[23]. The high coercive field increases the risk of dielectric breakdown; therefore poling could not be attained [24]. The substitution of Ba and

Sr into BFPT lowers the coercive field, enabling the measurement of the electromechanical response.
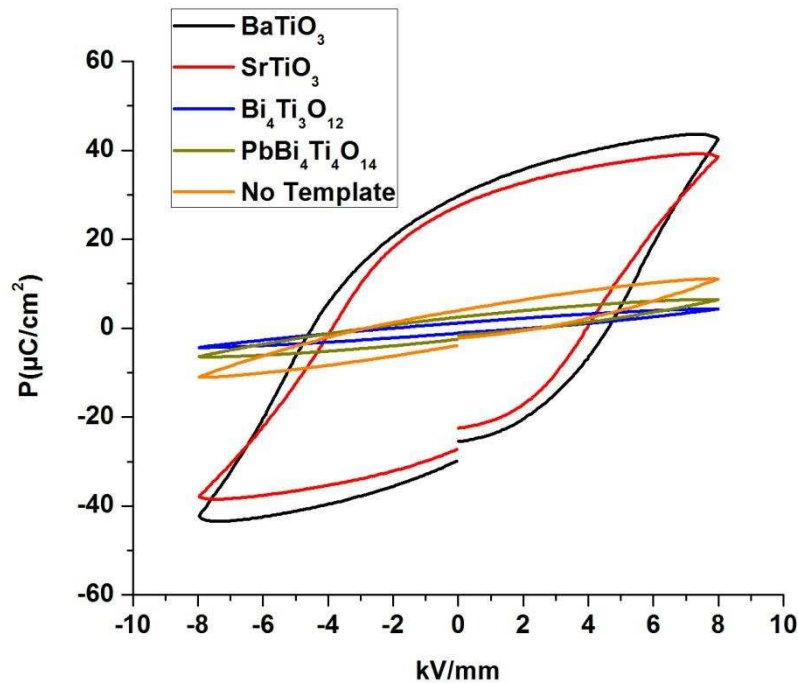
Figure 4. Comparison of ferroelectric hysteresis loops for 60:40BFPT processed using Aurivillius and perovskite templates as well as without templates.

The strain field plots (Fig.5) were used to determine the coercive field (Ec), taken as the minimum in strain. There is clear evidence of ferroelectricity for both $BaTiO_3$ and $SrTiO_3$ templated systems. The data shows Ec of 3.2 kV/mm, and a maximum strain of 0.15% for $SrTiO_3$ and coercive field of more than 6 kV/mm and a maximum strain of 0.10% for $BaTiO_3$ sample. The use of $SrTiO_3$ templates had a profound effect on ferroelectric properties, presumably as a result of Sr^{2+} doping into the lattice, indicating a higher level of reaction, or diffusion, for Sr^{2+} compared to Ba^{2+}.
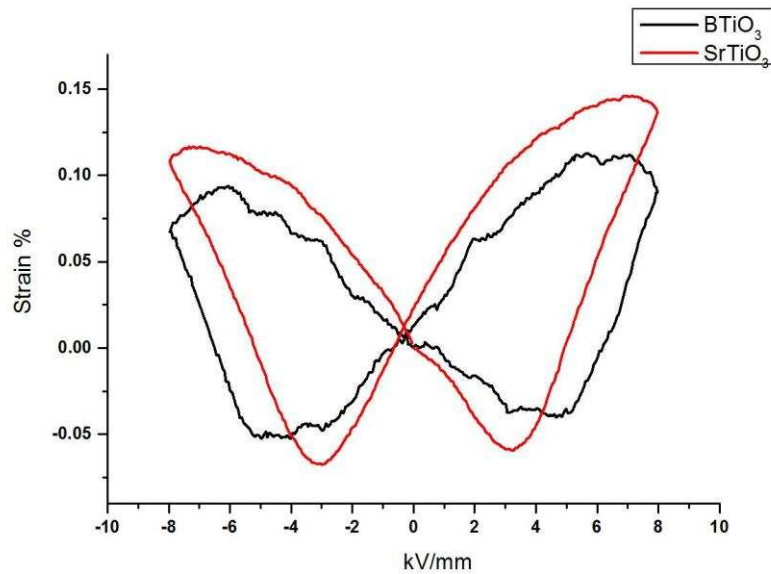
Figure 5. Comparison of strain field loops for 60:40BFPT processed with $BaTiO_3$ and $SrTiO_3$ templates.

Fig. 6 illustrates the frequency dependence of the permittivity (ε) and dielectric loss (δ) for the sample made from 10% $BaTiO_3$ templates. The permittivity data obtained from the cooling process. By increasing the frequency, permittivity decreases slightly. At high frequencies the dielectric dipoles enable to follow the applied electrical field which results in a lower permittivity value. At low frequencies sample becomes conductive.

At frequency of 1MHz, two maxima at 349 ^oC and 574 ^oC are observed. Recall from the EDX of BFPT made from $BaTiO_3$ (Fig.1), that there was a non-homogenous distribution of Ba^{2+}, suggesting that a compositional gradient is present, or a fraction of the initial $BaTiO_3$ was not consumed during the sintering process. Note that the T_c of $BaTiO_3$ is 130 °C, [25] and it is expected that remnant $BaTiO_3$ would be evidenced by a maximum in the dielectric response should occur at 130 °C if $BaTiO_3$ is present. A maximum is not observed, therefore it is concluded that partial substitution of the A site elements by Ba^{2+}, which could affect the Curie temperature of the final material.
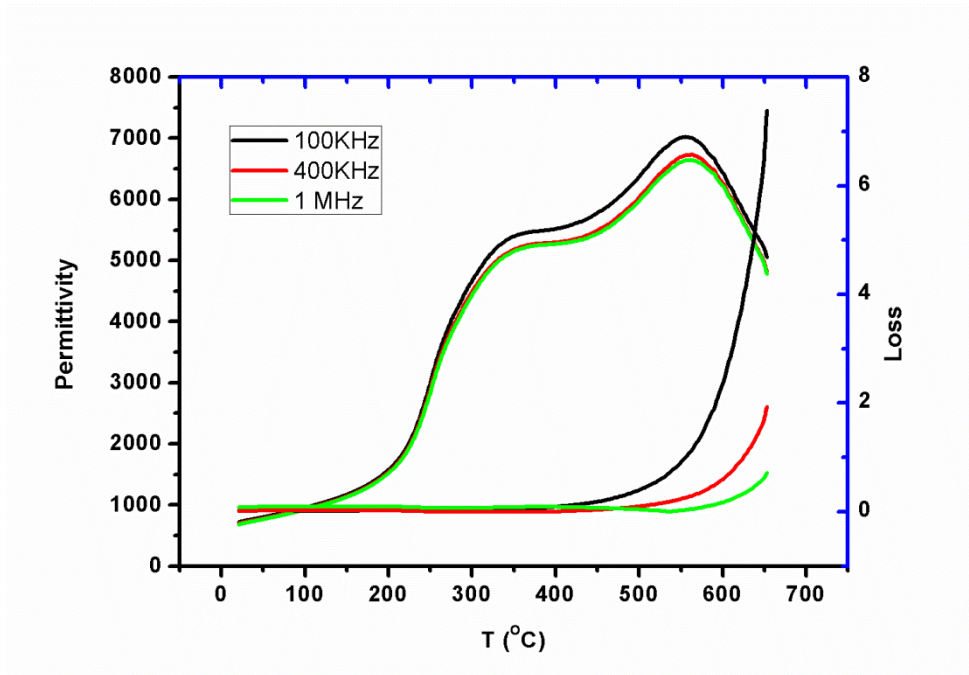
Figure 6. Relative permittivity (ε_r) and dielectric loss (δ) measured at different frequencies from room temperature to 650 °C for 60:40BFPT made using 10% $BaTiO_3$ templates.

Considering the permittivity data (table 1), the obtained maximum permittivity for both 60:40BFPT with and without $BaTiO_3$ are similar, whereas the c/a ratio in Ba-doped sample dramatically reduced in doped sample. This could be caused by possible Maxwell-Wanger polarization effect [26-29]. The existence of conductive phase could considerably influence the permittivity of the material. Fig.6 reveals the frequency dispersion of the material which could contribute to Maxwell-Wanger polarization effect. To investigate earlier assumption, some complementary technique such as in-situ TEM is required.

4. Conclusion

Although $Bi_4Ti_3O_{12}$, $PbBi_4Ti_4O_{15}$, $SrTiO_3$ have been used several times as template to synthesis textured ferroelectrics, in this study they did not impose texture on the 60:40BFPT matrix due to reaction between templates and matrix, as determined using SEM and XRD methods. However, using $BaTiO_3$ templates, some plate-like particles were observed after sintering. EDX data suggested that those plate-like particles were neither 60:40BFPT or the original composition, but somewhere in between, suggesting partial reaction.

Furthermore, synchrotron analysis reveals some degree of texture in the final Ba-doped BFPT. Samples were examined in two different directions, perpendicular and parallel to the cast direction. Considering the preferred direction of the templates and also casting direction some differences in intensities were observed. Although $BaTiO_3$ templates introduced Ba-doped 60:40BFPT, it was successful in generating texture, as determined using synchrotron measurement.

Using non Aurivillius and Aurivillius templates, generated at change in ferroelectric response. BFPT made by using non Aurivillius template exhibits a saturated PE loop which was not observed in ceramics made with Aurivillius templates. The similar story could be seen for $BaTiO_3$ and strain field / polarisation field exhibit the ferroelectricity behaviour. However, permittivity-temperature measurements suggest that the final product is Ba-doped 60:40BFPT.

References

1- S. E. Park and T. R. Shrout, "Ultrahigh strain and piezoelectric behavior in relaxor based ferroelectric single crystals ", J. Appl. Phys. 82 [4], 1804 (1997).

2- B. Noheda, J. A. Gonzalo, L. E. Cross, R. Guo, S. E. Park, D. E. Cox, and G. Shirane, "Tetragonal-to-monoclinic phase transition in a ferroelectric perovskite: The structure of $PbZr_{0.52}Ti_{0.48}O_3$", Phys. Rev. B 61[13], 8687 (2000).

3- F. Bai, N. Wang, J. Li, D. Viehland, P. M. Gehring, G. Xu, and G. Shirane, "X-ray and neutron diffraction investigations of the structural phase transformation sequence under electric field in $0.7Pb(Mg_{1/3}Nb_{2/3})$- $0.3PbTiO_3$ crystal", J. Appl. Phys. Rev. B: Condens. Matter 96[3], 1620 (2004).

4- M. K. Durbin, E. W. Jacobs, J. C. Hicks, and S. E. Park," In situ x-ray diffraction study of an electric field induced phase transition in the single crystal relaxor ferroelectric, 92% $Pb.Zn_{1/3}Nb_{2/3}.O_3$– 8% $PbTiO_3$", Appl. Phys. Lett. 74[19], 2848 (1999).

5- B. Noheda, D. E. Cox, G. Shirane, S. E. Park, L. E. Cross, and Z. Zhong, "Polarization Rotation via a Monoclinic Phase in the Piezoelectric 92% $PbZn_{1/3}Nb_{2/3}O_3$-8% $PbTiO_3$ ", Phys. Rev. Lett. 86[17], 3891 (2001).

6- H. Cao, F. M. Bai, N. G. Wang, J. F. Li, D. Viehland, G. Y. Xu, and G. Shirane," Intermediate ferroelectric orthorhombic and monoclinic MB phases in [110] electric-field-cooled $Pb,,Mg_{1/3}Nb_{2/3}O_3$– $30\%PbTiO_3$ crystals", Phys. Rev. B 72[6], 064104 (2005).

7- H. Cao, J.-F. Li, and D. Viehland, "Electric-field-induced orthorhombic to monoclinic MB phase transition in [111] electric field cooled $PbMg_{1/3}Nb_{2/3}O_3$–$30\%PbTiO_3$ crystals", J. Appl. Phys. 100[8], 084102 (2006).

8- Y. Venevzev, G.S. Zhdanov, S.P. Soloviev, H.V. Bezus, V.V. Ivanovav, S.A. Fedulov and A.G. Kapishev. "On crystal chemistry of perovskite- type compounds possessing special dielectric properties". Acta Crystallogr. , 13[12],1073-1073 (1960).

9- S.A. Fedulov, P.B. Ladyzhinskii, I.L. Pyatigorskaya and Y.N. Venevtsev. "Complete Phase Diagram of the $PbTiO_3$-$BiFeO_3$ System". Sov. Phys. Solid State, 6(2), 375-378 (1964).

10- S.A. Fedulov, Y.N. Venevtsev. "Investigation of the structure and dielectric properties of solid solutions of $(Pb,Sr)(Ti,Zr)O_3$". Sov. Phys. Solid State, 3(11), 2447-2450 (1962).

11- V. Sunder, A. Halliyal, A.M. Umarji. "Investigation of Tetragonal Distortion in the $PbTiO_3$ $BiFeO_3$ System by High-Temperature X-Ray-Diffraction". J. Mater. Res., 10(5),1301-1306 (1995).

12- T.P. Comyn, S.P. Mcbrid and A.J. Bell. "Processing and electrical properties of $BiFeO_3$-$PbTiO_3$ ceramics". Mater. Letter., 58(30), 3844-3846 (2004).

13- T. P. Comyn, T. J. Stevenson, M. Al-Jawad, G. André, A. J. Bell, R. Cywinski "Antiferromagnetic order in tetragonal bismuth ferrite–lead titanate", J. Magn. Magn. Mater., 323[21], 2533-2535 (2011).

14- T. Stevenson, T. P. Comyn, A. Daoud-Aladine, A. J. Bell, "Change in periodicity of the incommensurate magnetic order towards commensurate order in bismuth ferrite lead titanate", J Mag. Mag. Mater. , 322(22), L64-L67(2010).

15- M. Palizdar, T. P. Comyn, Y. Palizdar , and A. J. Bell., " Electron Backscattered Diffraction of MonoCrystalline Bismuth Titanate", J. Am. Ceram. Soc., 2010, 93(11), 3604-3606 (2010).

16- M. Palizdar, T. P. Comyn, and A. J. Bell, "Effect of different templates on reactive template grain growth of $BiFeO_3$-$PbTiO_3$", 2010 International Symposium on Applications of Ferroelectrics, 1-4 (2010).

17- M. Palizdar, T. P. Comyn, A. P. Kleppe, A. J. Jephcoat and A. J. Bell. "Reactive template grain growth of $BiFeO_3$-$PbTiO_3$ by using $Bi_4Ti_3O_{12}$, $PbBi_4Ti_4O_{15}$ and $SrTiO_3$ as templates", 2011 International Symposium on Applications of Ferroelectrics, 1-5 (2011).

18- J. Moon, E. Suvaci, A. Morrone, S. A. Costantino, J. H. Adair, 'Formation mechanisms and morphological changes during the hydrothermal synthesis of $BaTiO_3$ particles from a chemically

modified, amorphous titanium (hydrous) oxide precursor', J. Eu. Ceram. Soc., 23(12), 2153-2161 (2003).

19- K. H. Brosnan, S. F. Poterala, R. J. Meyer, S. Misture, G. L. Messing, **"Templated Grain Growth of <001> Textured PMN-28PT Using SrTiO$_3$ Templates"**, J. Am. Ceram. Soc., Special Issue: Ceramic Processing Science 92, S133–S139 (2009).

20- M. Palizdar, T. P. Comyn, S. F. Poterala, G. L. Messing, E. Suvaci, A. P. Kleppe, A. J. Jephcoat, A. J. Bell, "Synchrotron texture analysis of thick BiFeO$_3$-PbTiO$_3$ layers synthesised by tape casting using Aurivillius and non-Aurivillius templates," 2012 International Symposium on Applications of Ferroelectrics, 1-5 (2012).

21- T. Stevenson, "Magnetic and electric properties of bismuth ferrite lead titanate ceramics". PhD Thesis at University of Leeds , University of Leeds, 2011.[Thesis]

22- T. Hoshina, H. Kakemoto, T. Tsurumi, S. Wada, and M. Yashima, "Size and temperature induced phase transition behaviors of barium titanate nanoparticles", J. Appl. Phys., 99 (5), 1543 (2006).

23- T. P. Comyn, T. Stevenson and A. Bell, " Piezoelectric properties of BiFeO$_3$-PbTiO$_3$ ceramics", In: 2004 International Symposium on Applications of Ferroelectrics IEEE, 122-125 (2004).

24- T. P. Comyn, T. Stevenson and A. J. Bell, "Piezoelectric properties of BiFeO$_3$-PbTiO$_3$ ceramics". J. Phys. Iv, 128,13-17 (2005).

25- H. F. Kay, "Preparation and Properties of Crystals of Barium Titanate, BaTiO$_3$". Acta Crystallogr., 1(1-6), 229 (1948).

26- Z. Yua, and C. Ang, "Maxwell–Wagner polarization in ceramic composites BaTiO$_3$–.Ni$_{0.3}$Zn$_{0.7}$Fe$_{2.1}$O$_4$**",** J. Appl. Phys., 91(2), 794-797 (2002).

27- P. Lunkenheimer, S. Krohns, S. Riegg, S.G. Ebbinghaus, A. Reller, and A. Loidl, " Colossal dielectric constants in transition-metal oxides", Eur. Phys. J. Special Topics 180, 61‑89 (2010).

28- Jianjun Liu, Chun-Gang Duan, Wei-Guo Yin, W. N. Mei, R. W. Smith, and J. R. Hardy, "Large dielectric constant and Maxwell-Wagner relaxation in $Bi_{2/3}Cu_3Ti_4O_{12}$", J. Phys. Rev. B (**70),** 144106 (2004).

29- T. Prodromakis , C. Papavassiliou, "Engineering the Maxwell‑Wagner polarization effect", Appl. Surf. Sci., 255, 6989–6994(2009).